



Research Article

Fused Deposition Modelling Approach in Recycled Polypropylene/Aluminum Powder Composites for Sustainable Development

Manveer Rana and Mohit Kumar*

Department of Mechanical Engineering, Chandigarh University, Mohali, Punjab, India

Ranvijay Kumar

University Centre of Research and Development, Chandigarh University, Mohali, Punjab, India

* Corresponding author. E-mail: mohit.dhiman349@gmail.com DOI: 10.14416/j.asep.2024.07.009

Received: 18 April 2024; Revised: 6 June 2024; Accepted: 26 June 2024; Published online: 17 July 2024

© 2024 King Mongkut's University of Technology North Bangkok. All Rights Reserved.

Abstract

Polypropylene (PP) is a versatile and widely used thermoplastic polymer that has found its way into various aspects from packaging materials and consumer products to automotive components and industrial applications. However, this widespread use of polypropylene also presents a significant challenge in the disposal of polypropylene waste and its durability aspects. So, the fused deposition modeling (FDM) technique arises as compiling outcomes for recycling discarded PP waste to create functional products. The properties of FDM components produced from recycled polypropylene (r-PP) are notably inferior to those of virgin PP FDM counterparts. Hence, it becomes imperative to comprehend the substantial alterations that r-PP undergoes during successive extrusion processes, including chain scission, alterations in viscosity, and reductions in breaking strength. The incorporation of additives has emerged as a promising solution to enhance the performance of r-PP. In this context, the present study explores the development of a novel composite material by blending r-PP with aluminum powder. The combination of these materials leverages the sustainability benefits of r-PP and the excellent thermal and mechanical properties of aluminum, making it a promising candidate for a wide range of applications. The tensile results show a significant increase in Young's modulus for pre-heat treated composite specimen at 214 °C extrusion temperature. The SEM fractographic analysis confirms the homogenized distribution after pre-heat treatments. XRD results analyzed the degree of crystallinity in the composite specimens.

Keywords: Aluminum powder, Fused Deposition Modeling, Mechanical characterization, Recycled polypropylene, XRD

1 Introduction

Additive manufacturing, often referred to as 3D printing, has emerged as a revolutionary paradigm in modern manufacturing, offering unprecedented flexibility, customization, and efficiency [1]–[3]. Among the myriad of additive manufacturing techniques, Fused Deposition Modeling (FDM) stands out as a versatile and widely adopted method that has reshaped the landscape of prototyping, product development, and even end-use production [4]. The significance of FDM extends beyond its utilization in prototyping, encompassing a spectrum of industries

such as aerospace, healthcare, automotive, and consumer goods [5]. The FDM is the best additive manufacturing method that is suitable for thermoplastic materials such as polypropylene (PP), ABS, PLA, and a lot more [6]–[8]. Out of these, Polypropylene (PP), a versatile thermoplastic polymer, has long been a staple in various industries due to its excellent combination of mechanical properties, chemical resistance, and affordability [9]–[10]. However, the extensive use of polypropylene (PP) poses a considerable challenge in terms of waste disposal and the material's durability aspects [11], [12].



Inevitably, the life cycle conclusion of these objects contributes to a heightened accumulation of plastic waste, prompting the scientific community to explore innovative methods of waste management and valorization [13]–[17]. Recycling methods are considered more favorable compared to both landfilling and incineration, primarily due to the absence of recoverable materials at the conclusion of these processes [18]. Academic perspectives propose that stringent regulations imposed by the European Commission on the waste management of construction waste, vehicles, and electronic components urge industries reliant on composites to explore novel and efficient recycling approaches for their industrial waste [19]. Reuse is typically defined as the recycling of waste materials, often requiring multiple procedures for the recovery or valorization of waste into products applicable in diverse fields.

In this context, the FDM technique has emerged as a compelling solution, offering a pathway to recycle discarded PP material waste and embodying the principles of resource conservation and waste reduction [20]. While FDM presents an innovative approach to sustainable manufacturing, it is crucial to acknowledge that the properties of FDM components produced from recycled Polypropylene (r-PP) often fall short of those exhibited by their virgin PP counterparts. Numerous challenges, including inadequate mechanical properties stemming from potential thermal degradation, unregulated crystallinity, shrinkage caused by high fusion temperatures, and reduced durability, pose significant obstacles to the widespread adoption of recycled filaments in diverse engineering applications [20]. Understanding the substantial alterations that r-PP undergoes during successive extrusion processes is imperative, encompassing phenomena such as chain scission, alterations in viscosity, and reductions in breaking strength [21]. In light of these challenges, the integration of natural and synthetic fillers has surfaced as a promising avenue to enhance the performance of thermoplastics, particularly for applications in 3D printing. Different reinforcements, such as bakelite powder [22], ZrO₂ particles [23], wooden dust [22], Al₂O₃/SiC particles [24], biochar [25], and clothing fibers [26], have been employed to improve the stability and structural characteristics of FDM parts.

Moreover, very few studies have been reported that worked on the addition of fillers in r-PP. So, the present study delves into the development of a novel composite material achieved by blending r-PP with

aluminum powder. The rationale behind this approach lies in leveraging the sustainability benefits of r-PP and combining them with the outstanding thermal and mechanical properties of aluminum. The resulting composite material holds significant promise for a diverse array of applications within the additive manufacturing landscape. The physical and mechanical aspects of this novel composite material were through comprehensive assessments, including mechanical testing, scanning electron microscopy (SEM) and X-ray diffraction (XRD). In essence, this research contributes to the evolving discourse on sustainable additive manufacturing by exploring innovative solutions to enhance the performance of recycled materials.

2 Materials and Methods

The method of manufacturing the r-PP/Al based feedstock filaments involved the selection of the right proportion of Al loading in the r-PP matrix. The r-PP (pellets dia. 1.5-2.0 mm) was procured from the Batra Polymer Pvt. Ltd. Ludhiana, India and Al powder (size ~2 μm) was purchased from Shiva Chemical, Ludhiana, India. The loading of the Al in r-PP was determined by the observation based on MFI analysis. In the next stage, the feedstock filaments were manufactured using a single screw extruder machine (MakeL Felfil). Finally, the r-PP/Al composite filaments were characterized by tensile testing, scanning electron microscope (SEM), and X-ray diffraction (XRD) analysis.

The MFI of the r-PP/Al composites was determined using a melt flow indexer as per ASTM D1238 standard. The MFI of the r-PP/Al composites was measured by increasing the loading of Al in r-PP. The sample was prepared by mechanical mixing of Al with r-PP. The loading of 0–40% of Al was reinforced in the r-PP matrix and further, the flow pattern of the r-PP/Al composites was observed. As per the observation of MFI and flow pattern, the loading of Al was selected for filament manufacturing. In the next stage, the single screw extrusion process was carried out on r-PP/Al composites for manufacturing filament of diameter 1.75 ± 0.10 mm. The schematic of the preparation of feedstock filament is shown in Figure 1.

The extrusion was carried on the two types of r-PP/Al composites (a) non-heat treated (NHT) and (b) heat treated (HT) (Table 1). The pre-heat treatment can help in minimizing the defect in the extrusion process and promote uniform polymer-particle

distribution. The heat treatment was performed at 60 °C to remove the moisture content. Further, the temperature was varied between 208–214 °C based on

the dimensional accuracy observed in pilot experimentation. Figure 2 shows the manufactured r-PP/Al filaments.

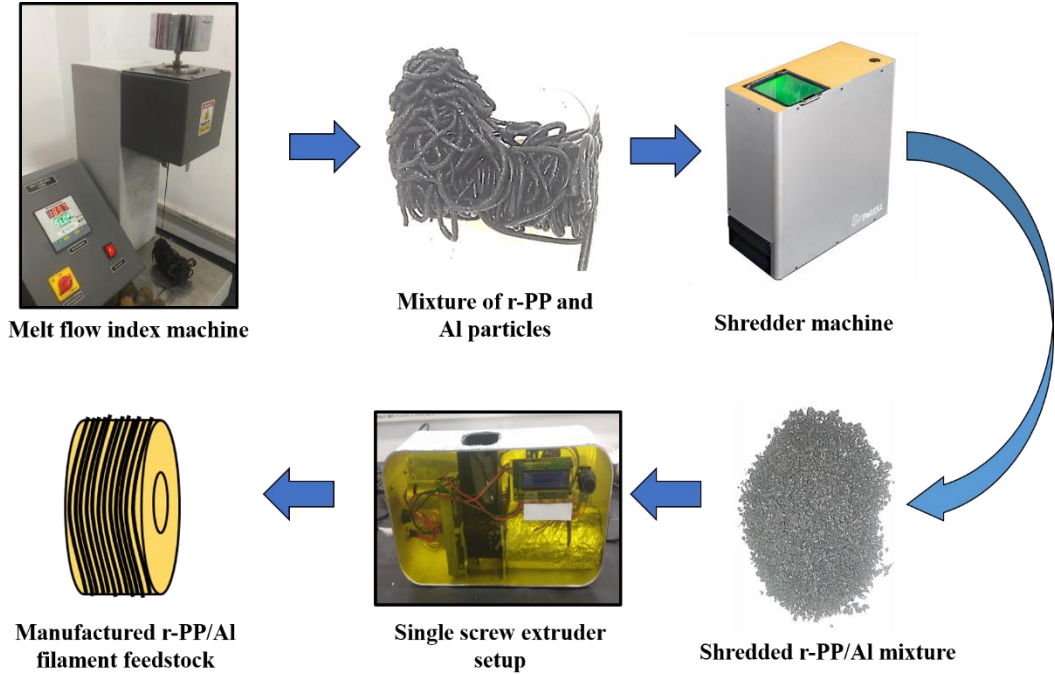


Figure 1: Schematic process of filament manufacturing.



Figure 2: Manufactured filaments of r-PP and r-PP/Al composites.

Table 1: Experimental condition for filament manufacturing.

Specimen No.	Processing type	Temperature (°C)
1	NHT	208
2	NHT	210
3	NHT	212
4	NHT	214
5	HT	208
6	HT	210
7	HT	212
8	HT	214

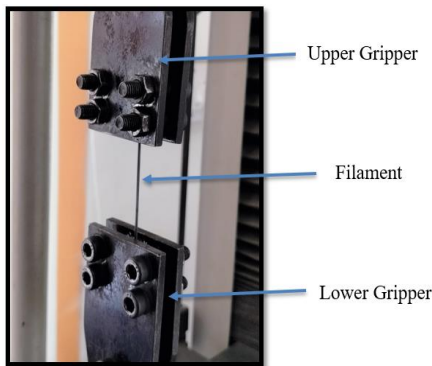


Figure 3: Tensile testing setup on UTM machine.

2.1 Material characterization

The manufactured feedstock filaments were subjected to tensile loading for measurement of strength at peak, peak strain, and Young’s modulus. The tensile test was performed on a universal testing machine (Make: Shanta Engineering; capacity: 5000N) at the strain rate of 20 mm/min as shown in Figure 3. The test was performed at room temperature.

The SEM (Make: Jeol; Model: JSM-IT500) was used to observe the fracture pattern and defects of the r-PP/Al composite feedstock filament undergoing tensile testing. The SEM was integrated with energy-



dispersive X-ray spectroscopy (EDS) for element analysis. The XRD analysis on the r-PP/Al composites was performed using the Cu-K α radiation ($\lambda = 1.54060$) in the range of 5–100°. The degree of crystallinity was investigated using the XRD analysis.

3 Results and Discussion

3.1 Optimization of Al powder wt. % in r-PP

The optimization of the desired wt.% of Al powder in the r-PP was carried out through the MFI method. The results obtained by mixing different wt.% of Al powder in r-PP are given in Table 2. Through obtained MFI values, it can be seen that by incorporating up to 5 wt.% of Al in r-PP, the MFI value hardly changes and the surface of the obtained r-PP/Al composite was smooth. After incorporating more Al powder up to 15 wt.%, the MFI values increased to 9.921 g/10min (9.53%) as compared to virgin r-PP composite. This can be due to the fact that the addition of Al particles can act as nucleating agents, promoting uniform melt flow and reducing viscosity, which leads to higher MFI values [27]. Moreover, the addition of Al powder up to 25 wt.%, results in a reduction in MFI values and increases the tendency of pores generation in the r-PP/Al composites. At 30 wt.%, due to the pores, the surface becomes rough as observed by visual inspection. Further, at 35 wt.%, the breakage in the composite was observed and more addition of Al powder resulted in choked and degraded composites.

Table 2: Visual observation of different wt.% of Al powder in r-PP.

S.No.	r-PP (%)	Al powder (wt.%)	MFI (g/10min)	Observations
1	100	0	9.058	Smooth
2	95	5	9.064	Smooth
3	90	10	9.729	MFI increased
4	85	15	9.921	MFI increased
5	80	20	9.199	Pore generated
6	75	25	9.040	Pore increased
7	70	30	8.982	Roughness due to pores
8	65	35	8.169	Breakage observed
9	60	40	-	Degraded and choked

From the results, the optimized quantity of Al powder was found to be 15 wt.% giving the maximum MFI value and a smooth surface. So, the final feedstock filaments were prepared by 15 wt.% added

Al powder in r-PP and characterized on the basis of their mechanical and physical aspects.

3.2 Tensile testing of r-PP/Al composites

A tensile test was conducted on the eight experimental variations (Table 1) of r-PP/Al composites for their tensile strength and modulus properties. The results of strength at peak and Young's modulus are shown in Table 3. The composite specimens 1–4 were of the non-heat treated (NHT) category and composite specimens 5–8 were given pre-heat treatment at 60 °C for 60 min. The properties obtained for these specimens were also compared with the virgin r-PP composites.

Table 3: Tensile characterization of r-PP/Al composites.

S.No.	Strength at peak (MPa)	Peak strain (mm/mm)	Young's modulus (MPa)
1	8.94	0.0882	101.360
2	12.02	0.0966	124.430
3	10.57	0.0756	139.814
4	9.15	0.0630	145.238
5	10.19	0.0714	142.717
6	8.15	0.0548	148.722
7	8.74	0.0588	148.639
8	9.36	0.0504	185.714

The results show that the tensile strength at peak for NHT specimens firstly increases up to 210 °C extrusion temperature, then starts decreasing with further increase in temperature. Specimen 2 (NHT, 210 °C) shows the best tensile strength at the peak which is approx. 69% higher than the virgin r-PP composite. The reduction in strength in specimens 3 and 4 was due to the Al particle agglomerate formation and extrusion defects [28]. Likewise, for HT specimens, the strength at peak for Specimen 5 (HT, 208 °C) was the best, which was approx. 43% higher than the virgin r-PP composite. The modulus properties were also assessed and it was found that out of all the composite specimens, specimen 8 (HT, 214 °C) gives the best modulus value of 185.714 MPa. This significant increase in the young's modulus may be due to the fact that pre-heat treatment allows to reduce the extrusion defects and results in better homogenization of Al particles in r-PP [29]. The overall increase in modulus was observed to be 86% as compared to virgin r-PP composite specimen.

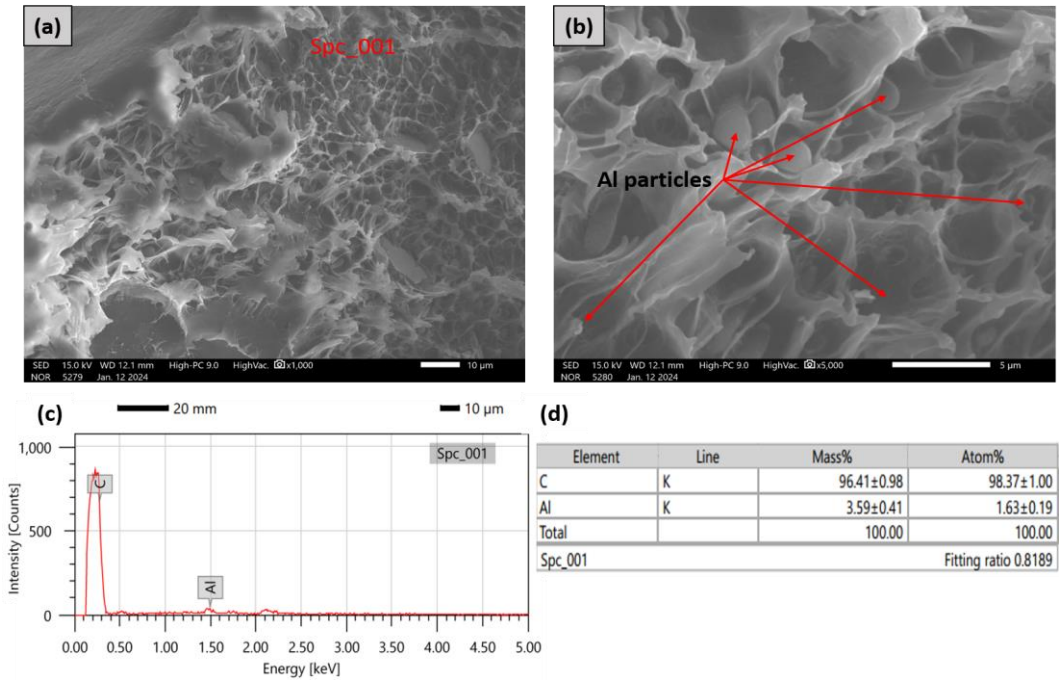


Figure 4: SEM and EDS analysis of r-PP/Al composite specimen 1 (NHT, 208 °C) showing (a) fracture surface at 1000X, (b) fracture surface with visible Al particles at 5000X, (c) Intensity (counts) vs Energy (keV) graph in EDS and (d) Elemental table showing C and Al content from EDS.

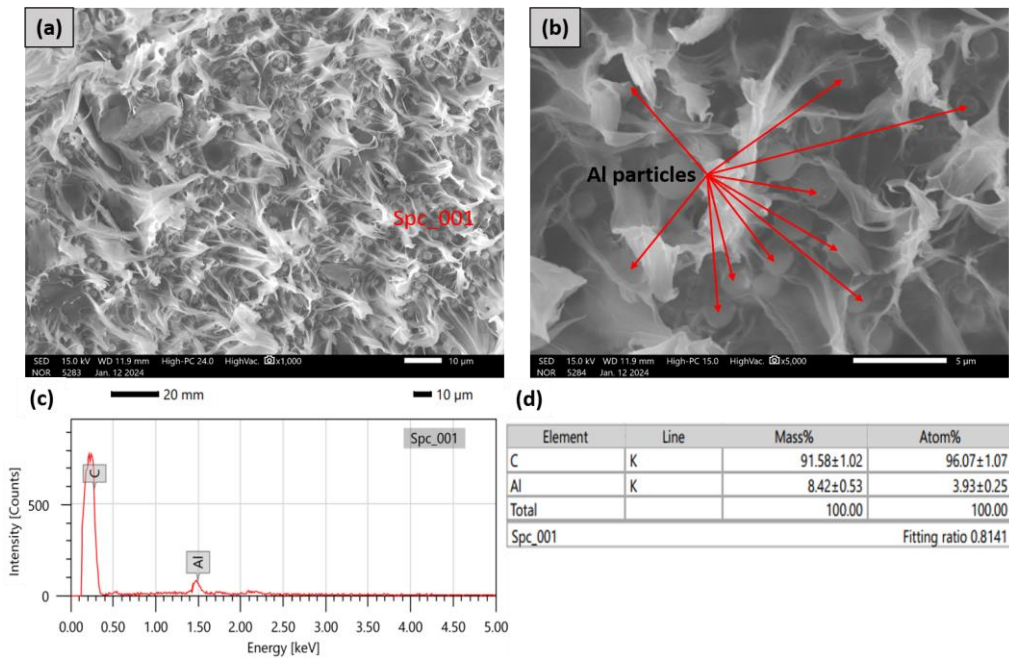


Figure 5: SEM and EDS analysis of r-PP/Al composite analysis of specimen 8 (HT, 214 °C) showing (a) fracture surface at 1000X, (b) fracture surface with visible Al particles at 5000X, (c) Intensity (counts) vs Energy (keV) graph in EDS and (d) Elemental table showing C and Al content from EDS.

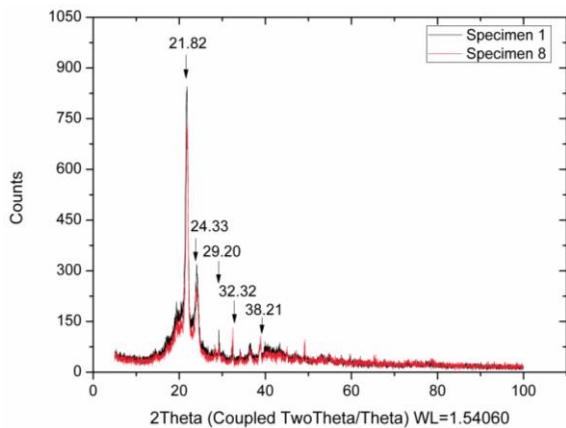


Figure 6: XRD results of specimen 1 (NHT, 208 °C) and specimen 8 (HT, 214 °C).

3.3 SEM analysis

The fractographic analysis for failed tensile specimens was conducted on specimen 1 (NHT, 208 °C) and specimen 8 (HT, 214 °C) having the lowest and highest Young's modulus in all configurations. Figure 4 shows the SEM-EDS results from specimen 1 (NHT, 208 °C) and Figure 5 shows the SEM-EDS results from specimen 8 (HT, 214 °C).

The fractured surfaces shown in Figure 4(a) and Figure 5(a) showed a rather ductile failure on the specimens. An excellent interlayer fusion can be seen between the PP and Al particles after extrusion, which corresponds to good interfacial bonding. As such, this could drive into high mechanical performance composite specimens with a potential enhancement and reinforcement of their mechanical properties due to the presence of Al particles [28]. In both Figure 4(b) and Figure 5(b), Al particles can be spotted clearly in the r-PP composite. It can be observed that the Al particles distribution was not homogenized and micro-aggregates presence can be noticed (Figure 4(b)). This may be due to the increased polymer melt viscosity hampering the inhomogeneous mixing of Al particles in r-PP [30]. The validation was remarked from the EDS results (from Figure 4(c) and (d)) confirming only 3.59 wt.% of Al in a specimen. Likewise, from Figure 5(b), it was noticed that Al particles are equally distributed within the r-PP, justifying the best Young's modulus results. The EDS (from Figure 5(c) and (d)) validated the presence of 8.42 wt.% of Al in r-PP, confirming the good homogenized distribution of Al particles. This can be due to the pre-heat treatment process which reduces the chances of agglomerates and promotes good r-PP/Al distribution.

The fractured surfaces shown in Figure 4(a) and Figure 5(a) showed a rather ductile failure on the specimens. An excellent interlayer fusion can be seen between the PP and Al particles after extrusion, which corresponds to good interfacial bonding. As such, this could drive into high mechanical performance composite specimens with a potential enhancement and reinforcement of their mechanical properties due to the presence of Al particles [28]. In both Figure 4(b) and Figure 5(b), Al particles can be spotted clearly in the r-PP composite. It can be observed that the Al particles distribution was not homogenized and micro-aggregates presence can be noticed (Figure 4(b)). This may be due to the increased polymer melt viscosity hampering the inhomogeneous mixing of Al particles in r-PP [30]. The validation was remarked from the EDS results (from Figure 4(c) and (d)) confirming only 3.59 wt.% of Al in a specimen. Likewise, from Figure 5(b), it was noticed that Al particles are equally distributed within the r-PP, justifying the best Young's modulus results. The EDS (from Figure 5(c) and (d)) validated the presence of 8.42 wt.% of Al in r-PP, confirming the good homogenized distribution of Al particles. This can be due to the pre-heat treatment process which reduces the chances of agglomerates and promotes good r-PP/Al distribution.

3.4 XRD analysis

XRD analysis was done to estimate the degree of crystallinity in the r-PP/Al composite specimens. Figure 6 presents the XRD results for Specimen 1 (NHT, 208 °C) and Specimen 8 (HT, 214 °C), Both specimens provide the proofs of crystallinity due to the presence of r-PP. It can be seen that the peaks at 32.32 and 38.21 show the presence of Al particles in the composite. The Peak of specimen 8 is higher than specimen 1, confirming the more wt.% of Al in r-PP composites and more homogenized distribution [31]. The higher steep peaks were observed in specimen 8 as compared to specimen 1, which means more crystallinity in specimen 8, confirmed by higher Young's modulus values in tensile testing.

4 Conclusions

The present study is based on the manufacturing of novel r-PP/Al feedstock composite filament for applications such as packaging materials, automotive components (interior trim parts and dashboard panel), electrical enclosures, junction boxes, and building

materials (pipes and fittings). The different experimental sets i.e., pre-heat treated and non-heat treated at different extrusion temperatures were used. The r-PP/Al composites were characterized by tensile testing, scanning electron microscope (SEM), and X-ray diffraction (XRD) analysis. The optimized wt.% of Al powder in r-PP is found to be 15 wt.% giving the maximum MFI value and a smooth surface. Incorporating Al particles serves as nucleation sites, fostering consistent melt flow and decreasing viscosity, consequently yielding elevated MFI values and smooth surfaces. The young's modulus properties are significantly increased for pre-heat treated specimens at 214 °C extrusion temperature. The reason being enhanced polymer alignment, improved filler dispersion and improved interfacial bonding at 214 °C. This further shows that feedstock composite for pre-heat treated conditions at 214 °C extrusion temperature can be used for product development. SEM and XRD results confirm the homogenized distribution of Al particles in r-PP for the composite specimen (HT, 214 °C), contributing to significant modulus properties. This can be attributed to the pre-heat treatment process, which minimizes agglomeration and encourages a uniform distribution of r-PP/Al throughout the material.

Acknowledgments

The authors are grateful to Department of Science and Technology (DST), India (Grant Number: SP/YO/2021/2514) for financial support.

Author Contributions

M.R.: conceptualization, investigation, editing; M.K.: investigation, methodology, writing an original draft; R.K.: writing—reviewing and editing.

Conflicts of Interest

The authors declare no conflict of interest.

References

- [1] S. C. Ligon, R. Liska, J. Stampfl, M. Gurr, and R. Mülhaupt, "Polymers for 3D printing and customized additive manufacturing," *Chemical Reviews*, vol. 117, no. 15, pp. 10212–10290, 2017.
- [2] S. S. Alghamdi, S. John, N. R. Choudhury, and N. K. Dutta, "Additive manufacturing of polymer materials: Progress, promise and challenges," *Polymers*, vol. 13, no. 5, p. 753, 2021.
- [3] L. J. Tan, W. Zhu, and K. Zhou, "Recent progress on polymer materials for additive manufacturing," *Advanced Functional Materials*, vol. 30, no. 43, 2020, Art. no. 2003062.
- [4] A. D. Mazurchevici, D. Nedelcu, and R. Popa, "Additive manufacturing of composite materials by FDM technology: A review," *Indian Journal of Engineering and Materials Sciences (IJEMS)*, 2020, doi: 10.56042/ijems.v27i2.45920.
- [5] S. C. Daminabo, S. Goel, S. A. Grammatikos, H. Y. Nezhad, and V. K. Thakur, "Fused deposition modeling-based additive manufacturing (3D printing): Techniques for polymer material systems," *Materials Today Chemistry*, vol. 16, 2020, Art. no. 100248.
- [6] W. Abd-Elaziem, M. Khedr, A. E. Abd-Elaziem, M. M. A. Allah, A. A. Mousa, H. M. Yehia, and M. A. A. El-Baky, "Particle-reinforced polymer matrix composites (PMC) fabricated by 3D printing," *Journal of Inorganic and Organometallic Polymers and Materials*, vol. 33, no. 12, pp. 3732–3749, 2023.
- [7] M. Baechle-Clayton, E. Loos, M. Taheri, and H. Taheri, "Failures and flaws in fused deposition modeling (FDM) additively manufactured polymers and composites," *Journal of Composites Science*, vol. 6, no.7, p. 202, 2022.
- [8] S. Mani, A. Kasi, R. Guruswamy, K. B. Nilagiri Balasubramanian, and A. Pandian, "Effect of post-processing treatment on 3D-printed polylactic acid parts: Layer interfaces and mechanical properties," *International Journal of Materials Research*, vol. 114, no. 10–11, pp. 999–1005, 2023.
- [9] H. A. Maddah, "Polypropylene as a promising plastic: A review," *American Journal of Polymer Science*, vol. 6, no. 1, pp. 1–11, 2016.
- [10] O. S. Carneiro, A. F. Silva, and R. Gomes, "Fused deposition modeling with polypropylene," *Materials & Design*, vol. 83, pp. 768–776, 2015.
- [11] R. V. Moharir and S. Kumar, "Challenges associated with plastic waste disposal and allied microbial routes for its effective degradation: A comprehensive review," *Journal of Cleaner Production*, vol. 208, pp. 65–76, 2019.
- [12] N. Evode, S. A. Qamar, M. Bilal, D. Barceló, and H. M. Iqbal, "Plastic waste and its management strategies for environmental sustainability," *Case Studies in Chemical and Environmental Engineering*, vol. 4, 2021, Art. no. 100142.
- [13] M. Kumar, J. S. Saini, H. Bhunia, and S. R. Chowdhury, "Aging of bolted joints prepared



- from electron-beam-cured multiwalled carbon nanotube-based nanocomposites with variable torques,” *Polymer Composites*, vol. 42, no. 8, pp. 4082–4104, 2021.
- [14] M. Kumar, J. S. Saini, and H. Bhunia, “Performance of mechanical joints prepared from carbon-fiber-reinforced polymer nanocomposites under accelerated environmental aging,” *Journal of Materials Engineering and Performance*, vol. 29, pp. 7511–7525, 2020.
- [15] R. Phiri, S. M. Rangappa, S. Siengchin, and D. Marinkovic, “Agro-waste natural fiber sample preparation techniques for bio-composites development: methodological insights,” *Facta Universitatis, Series: Mechanical Engineering*, vol. 21, no. 4, pp. 631–656, 2023.
- [16] S. K. Palaniappan, M. K. Singh, S. M. Rangappa, and S. Siengchin, “Eco-friendly biocomposites: A step towards achieving sustainable development goals,” *Composites*, vol. 7, no. 12, pp. 1–3, 2023.
- [17] I. Suyambulingam, S. M. Rangappa, and S. Siengchin, “Advanced materials and technologies for engineering applications,” *Applied Science and Engineering Progress*, vol. 16, no. 3, pp. 6760–6760, 2023, doi: 10.14416/j.asep.2023.01.008.
- [18] Y. C. Jang, G. Lee, Y. Kwon, J. H. Lim, and J. H. Jeong, “Recycling and management practices of plastic packaging waste towards a circular economy in South Korea,” *Resources, Conservation and Recycling*, vol. 158, 2020, Art. no. 104798.
- [19] S. Gharde and B. Kandasubramanian, “Mechanochemical and chemical recycling methodologies for the fibre reinforced plastic (FRP),” *Environmental Technology & Innovation*, vol. 14, 2019, Art. no. 100311.
- [20] V. Mishra, S. Negi, and S. Kar, “FDM-based additive manufacturing of recycled thermoplastics and associated composites,” *Journal of Material Cycles and Waste Management*, vol. 25, no. 2, pp. 758–784, 2023.
- [21] A. Al Rashid and M. Koc, “Additive manufacturing for sustainability and circular economy: Needs, challenges, and opportunities for 3D printing of recycled polymeric waste,” *Materials Today Sustainability*, 2023, Art. no. 100529.
- [22] K. Chawla, J. Singh, and R. Singh, “On recyclability of thermosetting polymer and wood dust as reinforcement in secondary recycled ABS for nonstructural engineering applications,” *Journal of Thermoplastic Composite Materials*, vol. 35, no. 7, pp. 913–937, 2022.
- [23] R. Singh, R. Kumar, S. Tiwari, S. Vishwakarma, S. Kakkar, V. Rajora, and S. Bhatoa, “On secondary recycling of ZrO₂-reinforced HDPE filament prepared from domestic waste for possible 3-D printing of bearings,” *Journal of Thermoplastic Composite Materials*, vol. 34, no. 9, pp. 1254–1272, 2021.
- [24] P. Bedi, R. Singh, and I. P. S. Ahuja, “Effect of SiC/Al₂O₃ particle size reinforcement in recycled LDPE matrix on mechanical properties of FDM feed stock filament,” *Virtual and Physical Prototyping*, vol. 13, no. 4, pp. 246–254, 2018.
- [25] M. Idrees, S. Jeelani, and V. Rangari, “Three-dimensional-printed sustainable biochar-recycled PET composites,” *ACS Sustainable Chemistry & Engineering*, vol. 6, no. 11, pp. 13940–13948, 2018.
- [26] I. A. Carrete, P. A. Quiñonez, D. Bermudez, and D. A. Roberson, “Incorporating textile-derived cellulose fibers for the strengthening of recycled polyethylene terephthalate for 3D printing feedstock materials,” *Journal of Polymers and the Environment*, vol. 29, pp. 662–671, 2021.
- [27] H. Junaedi, M. Baig, A. Dawood, E. Albahkali, and A. Almajid, “Effect of the matrix melt flow index and fillers on mechanical properties of polypropylene-based Composites,” *Materials*, vol. 15, no. 21, 2022, Art. no. 7568.
- [28] M. R. Parida, S. Mohanty, M. Biswal, S. K. Nayak, and S. Rai, “Influence of aluminum trihydrate (ATH) particle size on mechanical, thermal, flame retardancy and combustion behavior of polypropylene composites,” *Journal of Thermal Analysis and Calorimetry*, vol. 148, no. 3, pp. 807–819, 2023.
- [29] S. Siraj, A. H. Al-Marzouqi, M. Z. Iqbal, and W. Ahmed, “Impact of micro silica filler particle size on mechanical properties of polymeric based composite material,” *Polymers*, vol. 14, no. 22, 2022, Art. no. 4830.
- [30] O. Meziane, A. Bensedira, and M. Guessoum, “Rheological, mechanical, and morphological behaviour of polypropylene composites reinforced with ultrafine kaolinite particles,” *Matériaux & Techniques*, vol. 112, no. 1, p. 105, 2024.
- [31] E. D. S. B. Ferreira, C. B. B. Luna, E. M. Araujo, D. D. Siqueira, and R. M. R. Wellen, “Polypropylene/wood powder composites: Evaluation of PP viscosity in thermal, mechanical, thermomechanical, and morphological characters,” *Journal of Thermoplastic Composite Materials*, vol. 35, no. 1, pp. 71–92, 2022.